



HAL
open science

Engineering the electro-optic effect in HfO₂ and ZrO₂ through strain and polarization control

Francesco Delodovici, Cassidy Atkinson, Ran Xu, Pierre-Eymeric Janolin, S
Pamir Alpaya, Charles Paillard

► **To cite this version:**

Francesco Delodovici, Cassidy Atkinson, Ran Xu, Pierre-Eymeric Janolin, S Pamir Alpaya, et al..
Engineering the electro-optic effect in HfO₂ and ZrO₂ through strain and polarization control. Journal
of Applied Physics, 2023, 134, 10.1063/5.0158909 . hal-04198450

HAL Id: hal-04198450

<https://centralesupelec.hal.science/hal-04198450>

Submitted on 7 Sep 2023

HAL is a multi-disciplinary open access archive for the deposit and dissemination of scientific research documents, whether they are published or not. The documents may come from teaching and research institutions in France or abroad, or from public or private research centers.

L'archive ouverte pluridisciplinaire **HAL**, est destinée au dépôt et à la diffusion de documents scientifiques de niveau recherche, publiés ou non, émanant des établissements d'enseignement et de recherche français ou étrangers, des laboratoires publics ou privés.

Engineering the electro-optic effect in HfO₂ and ZrO₂ through strain and polarization control

Francesco Delodovici,¹ Cassidy Atkinson,² Ran Xu,¹ Pierre-Eymeric Janolin,¹ S. Pamir Alpay,^{2,3} and Charles Paillard^{1,4}

¹*Université Paris-Saclay, CentraleSupélec, CNRS, Laboratoire SPMS, 91190, Gif-sur-Yvette, France*

²*University of Connecticut, Department of Materials Science and Engineering and Institute of Materials Science, CT 06269, Storrs, USA*

³*Department of Physics, University of Connecticut, CT 06269, Storrs, USA*

⁴*Department of Physics, University of Arkansas, Fayetteville, Arkansas 72701, USA*

(*Electronic mail: charles.paillard@centralesupelec.fr)

(*Electronic mail: francesco.delodovici@centralesupelec.fr)

(Dated: 6 July 2023)

The ability to control the optical properties of a material with an electric field has led to optical memory devices, communication systems, optical signal processing or quantum cryptography. Understanding electro-optic effects, especially in thin films, would improve the efficiency of these applications. In particular, the influence of epitaxial strains is of prime importance. In addition, the active control of these effects would be of great interest to tailor the material to the desired performance. Here, we demonstrate through first-principle calculations that the linear electro-optic response (Pockels effect) of two silicon-compatible ferroelectrics is stable with respect to bi-axial strain and that the electro-optic response can be strongly enhanced through the electrical control of the polarization. We attribute the former to the lack of optical phonon softening and a weak elasto-optic response and the latter to the externally-induced softening of a phonon of symmetry A_1 . Our results are readily applicable to other polar materials and show that the electro-optic effect can be efficiently engineered to meet the performance criteria of future technologies.

I. INTRODUCTION

Bulk ferroelectric materials are well known for their strong optical response to an external perturbation such as an electric field or strain¹. They have been at the center of wide research efforts to discover novel materials for applications in integrated photonic circuits. Electro-optic (EO) effects, which allow the modulation of the refractive index with low frequency electric fields, are particularly relevant in this regard. The optical index modulation can be linear (so-called Pockels effect²) or quadratic (Kerr effect^{3,4}) in the electric field.

The search for materials showing large EO coefficients is crucial to enhance the performances of current and future EO devices, such as optical fibers or electro-optic modulators^{1,5}. Until now, ferroelectric materials such as barium titanate (BaTiO₃) or lithium niobate (LiNbO₃) have been largely investigated and commercially used. In particular, owing to the proximity of a phase transition at room temperature, barium titanate exhibits some of the largest Pockels coefficient ever measured⁶⁻⁸. However, barium titanate integration in devices presents challenges, including strong degradation of its EO properties as the dimensions are reduced⁹. Lithium niobate on the other hand shows a weaker EO coupling coefficient (around 30 pm/V¹⁰) but has been successfully employed in communication applications¹¹. Thus, there is a strong urge to discover new EO materials showing large Pockels coefficients (which we also refer to as EO constants here) even when the materials dimensions are reduced. A recent study suggests substrate-induced strain as a possible way to engineer the EO effect in ferroelectric materials such as PbTiO₃ film¹². It was shown that large improvement in the EO constants results from optical phonon softening or enhanced piezoelectricity induced by bi-axial strain. Similarly, 2D ferroelectric materials have been predicted to exhibit Pockels coefficients on par with lithium niobate¹³.

A current ferroelectric material of significant interest is hafnium oxide HfO₂^{14,15}. It naturally exhibits ferroelectricity at the nanoscale¹⁶, possibly because ferroelectricity does not directly originate from the condensation of a primary polar soft mode as in ferroelectric perovskite oxides¹⁷. Ferroelectricity in hafnia is usually related to an orthorhombic *Pca*2₁ phase¹⁸⁻²¹ or a rhombohedral *R3m* phase²²⁻²⁴. HfO₂ is silicon compatible²⁵, and its promising endurance²⁶ and its relatively low cost of production make it a viable candidate for applications in ferroelectric memory devices. HfO₂ is therefore also a natural candidate to include in the search for outstanding EO materials for photonic applications on silicon. On the other hand, ZrO₂ shows similar crystal structures and electric properties with HfO₂. Moreover, Zr doping is widely employed to

enhances the stability of HfO₂ orthorhombic phase in thin films²⁷. Despite being of interest for its anti-ferroelectric properties^{28,29}, ZrO₂ polar orthorhombic phase has been recently observed in Ta-doped thin films³⁰. Therefore, ZrO₂ appears as natural benchmark to compare the properties of HfO₂. Recently, their EO properties have been investigated in thin-film samples^{31,32} reporting values of Pockels coefficients lower than those of lithium niobate, but still potentially interesting for applications. Specifically El Boutaybi *et al.*³² compared the *bulk* EO properties of HfO₂ with ZrO₂ and lithium niobate. The computed linear-EO effect coefficients for the orthorhombic phase *Pca2₁* are higher in ZrO₂ than in HfO₂: r_{33} and r_{13} , the largest and the smallest coefficients, are respectively 11 pm/V and -12 pm/V in ZrO₂ and 7 pm/V and -8 pm/V in HfO₂. On the other hand, the Pockels effect in the rhombohedral phase *R3m* is much weaker: the r coefficients are at least one order of magnitude smaller than the corresponding ones in the orthorhombic phase.

Epitaxial strains induced by the lattice mismatch with the substrate play a major role in the stabilization of hafnia ferroelectric phases^{18,33} together with doping³⁴⁻³⁶ and the presence of oxygen vacancies^{37,38}. As a result, most applications of ferroelectric HfO₂ involve thin film deposition, and thus the presence of in-plane strains and clamping by a substrate. It is thus crucial to understand the EO properties of strained HfO₂. We address this issue by means of *ab-initio* simulations, analyzing the effect of bi-axial strain on the EO properties of the polar phase of HfO₂ and the related polar compound ZrO₂ as a comparison. We investigate the various sources of the Pockels effect of hafnium oxide, namely the electronic, the ionic, and the cell responses. We show that the ionic contribution dominates the EO response and that the Pockels coefficients are remarkably stable within a reasonable range of epitaxial strains. Moreover, we suggest a promising way to engineer the optical properties of HfO₂ and ZrO₂ by controlling their polarization via an external voltage.

II. METHODS

The Pockels effect characterizes the change of refractive index, Δn_{ij} , linearly induced by an applied low-frequency electric field. It is formally described by a third order tensor r_{ijk} (the Pockels tensor), which relates the change in dielectric impermeability β_{ij} to the external electric field E_k ³⁹:

$$\Delta\beta_{ij} = \Delta\epsilon_{ij}^{-1} = \sum_k r_{ijk} E_k \quad (1)$$

where ϵ_{ij} is the total dielectric tensor and $\beta_{ij} = (n^{-2})_{ij}$ is the dielectric impermeability. n_{ij} is the refractive index. Due to the odd order of the Pockels tensor r_{ijk} , the Pockels effect only occurs in systems lacking an inversion symmetry, such as ferroelectrics.

The tensor r_{ijk} can be decomposed as^{39,40}:

$$r_{ijk} = r_{ijk}^{\text{el}} + r_{ijk}^{\text{ion}} + r_{ijk}^{\text{cell}}. \quad (2)$$

r_{ijk}^{el} describes the contribution to the Pockels effect of the valence electrons when interacting with E_k at clamped ion positions and cell shape. r_{ijk}^{ion} represents the contribution from the ion relaxation under an applied electric field. It can be decomposed in terms of the phonon modes³⁹: the contribution of one phonon mode α to the Pockels response depends on ω_α^{-2} (ω_α being the phonon frequency), its polarity p_m and Raman scattering efficiency α_m . Hence, engineering soft infrared and Raman-active phonon modes (either with strain¹² or temperature⁴⁰) is one way to design EO materials with large Pockels response. The term r_{ijk}^{cell} in Eq. 2 describes the response of the unit-cell shape relaxation generated by the piezo-electric effect and its consequence on the optical properties. It can be obtained as the contraction of the d piezo-electric tensor with the p elasto-optic tensor at zero electric field.

All the mentioned quantities can be obtained in the framework of Density Functional Theory (DFT) computations. Specifically, we employ Abinit^{41,42} to calculate *ab-initio* the EO properties of strained HfO₂ and ZrO₂. The norm-conserving pseudo-potentials available on PseudoDojo are used with 12 valence electrons for Hf and Zr, and 6 for O. We employed the Local Density Approximation (LDA) exchange-correlation functional⁴³, with a plane-wave cutoff of 60 Ha and a $7 \times 7 \times 7$ k-point mesh. Bi-axial strain is applied by fixing two lattice vectors and letting the atoms and the third lattice vector relax until the force acting on every atom is lower than 10^{-5} Ha/Bohr. The strain η scales the in-plane lattice constants of the relaxed orthorhombic phase by a factor $1 + \eta$.

III. RESULTS AND DISCUSSION

We first relax the $Pca2_1$ orthorhombic phase of HfO₂ and ZrO₂. Fig. 1 shows this crystal structure including 12 atoms per primitive cell. For each strained configuration of the $Pca2_1$ phase, we compute the clamped-ions electro-optical coefficients r_{ijk} , corresponding to $r_{ijk}^{\text{el}} + r_{ijk}^{\text{ion}}$ in Equation 2. The symmetries of the $Pca2_1$ space group⁴⁴ reduce the r_{ijk} tensor, written with Voigt's

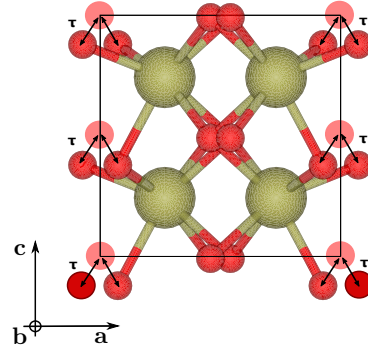


FIG. 1. The orthorhombic phase of HfO_2 : Hf atoms are reported in gold and the oxygen in red. The polarization axis lays along the c primitive vector. The pink spheres represent the oxygen high-symmetry coordinates when they are displaced from their ferroelectric positions by τ .

notation⁴⁵, to:

$$r_{ij} = \begin{bmatrix} 0 & 0 & r_{13} \\ 0 & 0 & r_{23} \\ 0 & 0 & r_{33} \\ 0 & r_{42} & 0 \\ r_{51} & 0 & 0 \\ 0 & 0 & 0 \end{bmatrix} \quad (3)$$

where $r_{13} = r_{113}$, $r_{23} = r_{223}$, $r_{33} = r_{333}$, $r_{42} = r_{232}$, $r_{51} = r_{311}$, with $r_{ijk} = r_{jik}$ due to intrinsic symmetry. In both HfO_2 and ZrO_2 , the magnitude of the largest Pockels coefficients (between 5 and 10 pm/V) is on par with those of commonly used EO materials such as lithium niobate (≈ 30 pm/V)³⁹. Specifically, our simulations at zero strain predict the largest (in magnitude) coefficient to be $r_{33(13)} = 5.3(-5.1)$ pm/V and $r_{33(13)} = 7.0(-7.2)$ pm/V for HfO_2 (respectively, ZrO_2). These agree well with the literature³².

Fig. 2 reports the strain dependence of the linear EO coefficients of HfO_2 and ZrO_2 . It reveals an overall weak dependence of the EO coefficients on the applied strain for both materials, independently on the direction of application. Most tensor components show an almost linear dependence with the in-plane strain η . Deviations from that linear behavior appear for r_{13} , r_{23} , and r_{33} (to smaller extent) when epitaxial strain is imposed along primitive vectors a , b and a , c . This shift from linearity is due to the superposition of non-linear strain dependence of specific phonon-mode contributions reported in Fig. 3 for HfO_2 . In the case of r_{33} , the non-linear contributions partially compensate producing a less obvious non-linear strain dependency. Similar features are

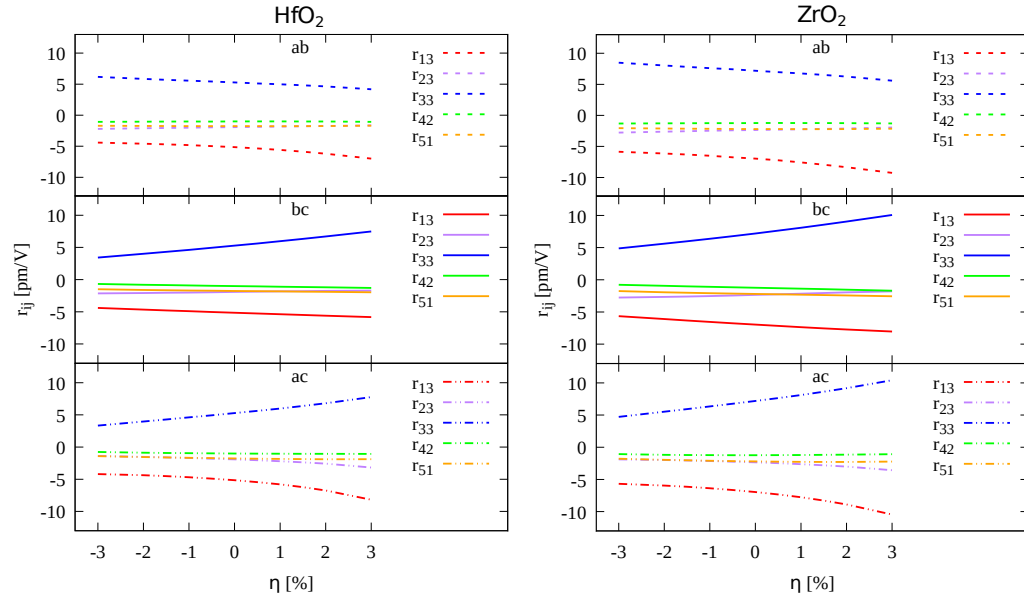


FIG. 2. Strain dependence of the Pockels coefficients r_{ij} for (left) HfO_2 and (right) ZrO_2 . The strain is applied along (top panel) the **a-b**, (middle panel) **b-c** and (lower panel) **a-c** primitive vectors. Each color represents a different coefficient: r_{13} in red, r_{23} in violet, r_{33} in blue, r_{42} in green, r_{51} in orange.

observed for ZrO_2 (see Supporting Information). Fig. 3 reports the decomposition of the largest (in magnitude) coefficients r_{13} and r_{33} of HfO_2 in terms of the electronic r^{el} and phonon-mode decomposed $r_{\text{m}}^{\text{ion}}$ contributions.

In both oxides, the sum of the terms $r_{\text{m}}^{\text{ion}}$ is invariably larger than the electronic contributions for the coefficients r_{13} , r_{23} , r_{33} . The valence electrons account for a minor part of the total EO effect: less than 23% of the total Pockels coefficient in HfO_2 and less than 30% in ZrO_2 . A similar situation can be found in most EO materials (LiNbO_3 , BaTiO_3 , PbTiO_3 , PZT, AlN/ScN superlattices or 2 dimensional ferroelectric materials^{12,13,39,46,47}). For the other two finite coefficients, r_{42} and r_{51} , the electron response may be responsible for more than half the value of the coefficients in both oxides. In this case, the dominant role of electron response is due to the reduced contribution of phonon modes and to their mutual compensations rather than to an enhancement of the electrons response itself. More information are reported in the Supplementary material. The low contribution from the electronic response to the EO effect may be a consequence of a general inverse relationship between the permittivity and the band gap⁴⁸. This inverse dependence can be traced back to the dependence of electronic susceptibility on the inverse of transition-states energy difference appearing at a first-order perturbation theory level. Both HfO_2 and ZrO_2 have

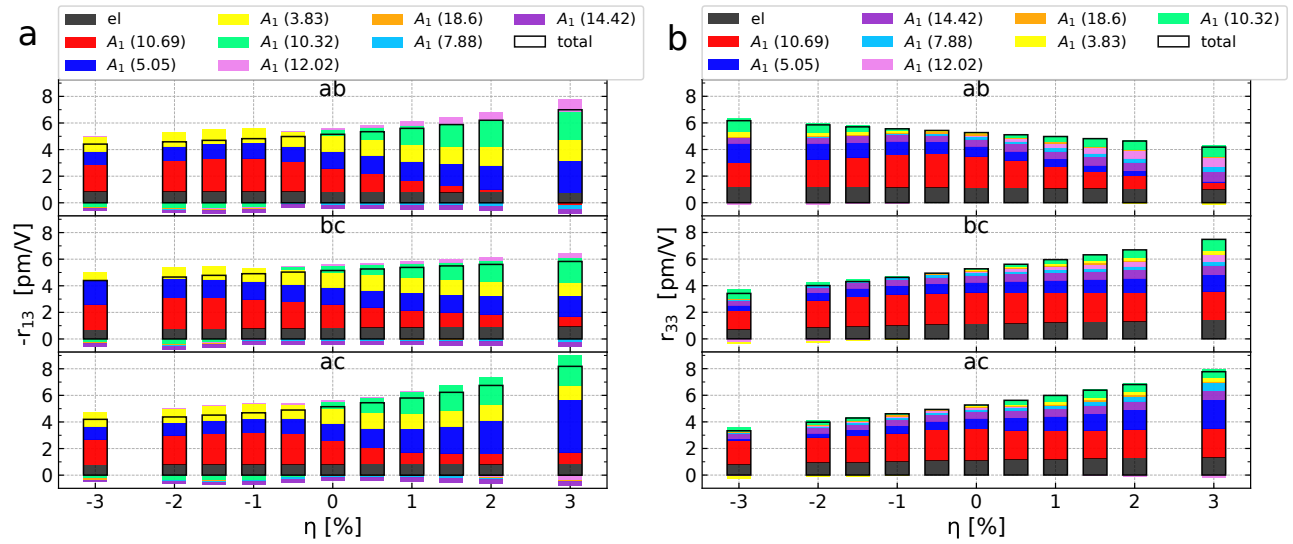


FIG. 3. Electronic and mode-decomposed ionic contributions to the (a) r_{13} and (b) r_{33} coefficients as a function of the applied strain for HfO_2 . Each colored bar corresponds to the contribution of a different phonon mode, which is labelled by its symmetry and frequency in the unstrained phase (in parenthesis, expressed in THz). The electronic contribution is represented in black. The top panel reports the effects of strain applied along **a-b** primitive vectors; the middle panel, along **b-c**; the bottom panel along **a-c**.

large electronic band gaps, ≈ 3.9 eV as predicted by our *ab-initio* simulations at the LDA level of approximation.

Despite this overall reduced role of the valence electron response, the changes in r_{ij}^{el} induced by the strain can be quite large: *e.g.* r_{33}^{el} increases by 66% in ZrO_2 and by 63% in HfO_2 as strain applied along **b** and **c** runs from compressive to tensile. The change in the large bandgap (around 5%, see Supplementary material) of HfO_2 and ZrO_2 partially accounts for these changes in contribution of r^{el} to the Pockels effect.

On the other hand, the ionic response represents the largest contribution to the Pockels coefficients. To reveal how the strain direction and intensity determine the optically-active mode contribution to the EO coefficients, we decompose r^{ion} on the lattice vibrations in HfO_2 and ZrO_2 . Both the oxides exhibit 33 optical phonon modes in the orthorhombic phase. Let us focus here on the case of HfO_2 . It has 8 optical phonons of B_2 symmetry, 9 with B_1 symmetry, 8 with A_2 symmetry and 8 have A_1 symmetry. All the optical modes are infrared- and Raman-active except those with B_1 symmetry, which are not coupled with the polarization. Therefore, all optical modes but those with B_1 symmetry contribute to the EO response of HfO_2 . Specifically, the A_1 modes

contribute to the $r_{13,23,33}$, the A_2 to r_{51} and the B_2 to r_{42} , as seen in Fig. 3 and in Supplementary material. The decomposition on the vibrational modes reveals the peculiar dependence of each mode's contribution on the strain state. Despite the strong dependency of some modes (see Supplementary material), the strain behaviour of various A_1 , A_2 , B_2 modes compensate, giving rise to an overall weak dependency of the Pockels coefficients on the strain intensity and direction of application. In addition, given the inverse relationship between the contribution of a phonon mode to the Pockels effect and its frequency³⁹, the remarkable stability of the Pockels coefficients with in-plane strain originates also from the absence of a strongly softening optical phonon mode. We report the phonon frequencies at Γ as a function of the strain in the Supplementary material.

So far, we have discussed the *clamped* linear EO response, *i.e.* without considering the response of the cell (third term in Eq. 2). Since HfO_2 and ZrO_2 are grown as thin films on substrates, the out-of-plane direction is, however, free to relax its lattice constant and angles to minimize the stress. We find that the EO response associated with those effects is negligible due to a very low elasto-optic response (see Supplementary material).

Due to the ferroelectric nature of orthorhombic phase of HfO_2 , one can imagine to play with the electrical polarization itself, *i.e.* by means of *electrical* engineering rather by *mechanical* engineering by substrate-induced strain. This can be achieved by controlling the electrostatic boundary conditions via the use of dielectric layers, as was demonstrated in negative capacitance experiments in other ferroelectrics^{49,50}, or by the application of bias electric fields. It is therefore of interest to clarify the relationship between the EO effects and the residual polarization of the system. Hereby, we consider the amplitude τ of the ferroelectric displacements, illustrated in Fig. 1, as a signature for the change of polarization in the polar phase. The high-symmetry $\text{Fm}\bar{3}\text{m}$ phase is taken as a reference and it is characterized by $\tau = 0$. $\tau = 1$ characterizes the relaxed, ferroelectric orthorhombic structure. We compute the EO coefficients as a function of frozen increasing ferroelectric displacement τ in the relaxed primitive-cell volume, from the high-symmetry cubic phase to the polar orthorhombic one. To assign a polarization value to each intermediate configuration we contracted the Born effective charge tensor of the ferroelectric phase with the vector of atomic displacements for each value of τ . The Born effective charge analysis leads to a value of $P \approx 46.8 \mu\text{C}/\text{cm}^2$ for the relaxed ferroelectric phase. This value underestimates our Berry-phase result by 18% ($P_{\text{Berry}} = 57.7 \mu\text{C}/\text{cm}^2$) (see the Supporting Information). Nonetheless, the effective charges provides a more intuitive framework to associate the ferroelectric displacements with the reduction of the polarization. Fig. 4 depicts the Pockels coefficients

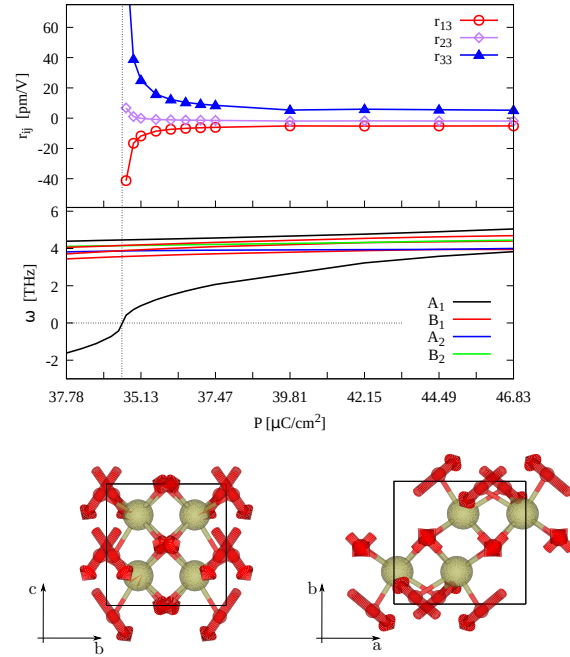


FIG. 4. **Top** The top panel reports the r_{13}, r_{23}, r_{33} coefficients as a function of the polarization P for HfO_2 . The bottom panel report the lowest phonon frequencies at Γ as a function of P . The softening mode is represented in black. **Bottom**, two views of the atomic displacements corresponding to the softening mode are reported. The Hf atoms are represented in gold, the oxygen atoms in red. The arrows represent the atomic displacements.

as a function of the polarization for HfO_2 . The reduction of the ferroelectric distortion induces the softening of a phonon of symmetry A_1 whose frequency in the relaxed ferroelectric phase is 3.83 (3.26) THz in $\text{HfO}_2(\text{ZrO}_2)$. This mode condenses for a value of $P \approx 34.65 \mu\text{C}/\text{cm}^2$ for HfO_2 and of $P \approx 41.15 \mu\text{C}/\text{cm}^2$ for ZrO_2 (see Supporting Information), corresponding to a 26% and 13% reduction of the value computed for the ferroelectric phase. Based on the computed total permittivity of these oxides ($\epsilon_{zz} \approx 20.62$ in HfO_2 and ≈ 25.26 in ZrO_2), we estimate the electric field needed to induce such phonon softening and then of the corresponding bias voltage for a film thickness of 5 nm⁵¹ to be 3.5 V for HfO_2 and 1.4 V for ZrO_2 . Note that the coercive fields in HfO_2 or ZrO_2 ultra-thin film are typically of the order of 1-2 MV/cm^{52,53}. Despite our estimated electric fields being larger than the coercive field in HfO_2 , other means of polarization control can be envisioned. For instance, research on negative capacitance suggests that combining HfO_2 or ZrO_2 with a stiff dielectric may frustrate the polarization^{49,50}, potentially enhancing the electro-optic response. As the ionic contribution to the Pockels effect depends on the inverse of the square of

the phonon frequency, this mode condensation induces a divergence in the EO coefficients. The ionic displacements describing the softening phonon are reported at the bottom of Fig. 4. They are non-trivial and can hardly be described in terms of tilting modes around the primitive vectors. We stress that, to the purpose of our theoretical analysis, the nature of the high-symmetry phase is not particularly relevant, as it is just a reference to examine the effects of controlling the polarization. The results would likely remain the same if we had also considered another high-symmetry phase as the reference, non-polar phase.

IV. CONCLUSION

In this work, we calculated the EO response of the polar orthorhombic phase of HfO_2 and ZrO_2 while constraining either (i) the in-plane strain, to mimic the mechanical interaction with a substrate or (ii) the polarization, to mimic the application of an external voltage bias.

The linear electro-optic response of the two oxides shows little dependence on an external mechanical action preserving the orthorhombic symmetry of the structure. The decomposition of the response in terms of electronic and ionic contributions allows to detect the dominant role played by the lattice dynamics over the electronic response. The lack of soft phonons in the considered range of strain prevents the lattice to provide a larger contribution to the EO response, in contrast to other ferroelectric materials such as PbTiO_3 , engineered to the edge of phase transitions by means of strain¹². This also implies that HfO_2 and ZrO_2 exhibit a remarkable stability of their EO response over a large range of strain. Smaller losses are also to be expected in these materials. The contribution of the unit cell response (unclamped part of the Pockels coefficients) is shown to be one to two orders of magnitude smaller than the electronic and ionic response. This traces back to a weak elasto-optical response and to its weak dependence on the applied strain. The external control of polarization instead provides another path to engineer the electro-optical response. Our results show that lowering the polarization while preserving the orthorhombic symmetry drives the system towards a dynamical lattice instability, as indicated by the softening of an optical phonon. As a result, a large enhancement of the EO response is to be expected in HfO_2 and ZrO_2 by the proper application of bias voltages. The control of polarization by means of an external voltage should be thought of in terms of a superposition of linear (Pockels) and non-linear (Kerr) effects, rather than a simple linear effect⁴⁷. Since the form factor³² of HfO_2 and ZrO_2 is larger than other ferroelectric materials, such as BaTiO_3 and PbTiO_3 ¹, we expect that these oxides will gain

traction in EO applications at the nanoscale. Compared to other EO materials such as perovskite oxides, they are compatible with integrated circuits based on silicon and their production cost is competitive.

This work demonstrates that the EO properties are conserved at the nanoscale, when bi-axial strain is present in epitaxially-grown HfO₂ or ZrO₂ films. Our results urge for experimental confirmations, as they shine light on aspects of HfO₂ and ZrO₂ which have not been deeply investigated yet, and as they potentially pave the route for new fields of application for these two oxides.

V. SUPPLEMENTARY MATERIALS

The supporting information contains the following: strain dependency of the electrons band gap; definition and analysis of the piezoelectric contribution to the EO effect; the strain dependence of the EO coefficient of ZrO₂; the decomposition in electronic and lattice contribution of the r_{13}, r_{33} EO coefficients for ZrO₂; the decomposition in electronic and lattice contribution of the r_{23}, r_{42}, r_{51} EO coefficients for HfO₂; the phonon frequencies at Γ as a function of the applied bi-axial strain for HfO₂ and ZrO₂; the atomic displacements corresponding to selected phonon modes; the dependence of the EO coefficients on P in ZrO₂; the procedure used to estimate the bias voltage; a comparison of the polarization of the polar phase of HfO₂ computed with Born effective charges and with Berry-phase method.

AUTHOR DECLARATIONS

Conflict of interest

The authors have no conflicts to disclose.

Authors contribution

Francesco Delodovici: Conceptualization (lead); Data curation (lead); Formal Analysis (lead); Visualization (lead); Writing – original draft (lead); Writing – review & editing (lead). **Cassidy Atkinson:** Data curation (equal); Writing – review & editing (equal). **Ran Xu:** Data curation (equal); Writing – review & editing (equal). **Pierre-Eymeric Janolin:** Conceptualization (equal); Writing – review & editing (equal). **S.Pamir Alpay:** Writing – review & editing (equal), Su-

pervision(equal); **Charles Paillard**: Conceptualization (lead); Writing – review & editing (lead); Supervision(lead).

Data Availability Statement

The data that support the findings of this study are available within the article and its supplementary material.

REFERENCES

- ¹D. Sando, Y. Yang, C. Paillard, B. Dkhil, L. Bellaiche, and V. Nagarajan, “Epitaxial ferroelectric oxide thin films for optical applications,” *Applied Physics Reviews* **5**, 041108 (2018).
- ²“Frontmatter and index,” in *Fundamentals of Photonics* (John Wiley & Sons, Ltd, 1991).
- ³J. Kerr, “XI. a new relation between electricity and light: Dielectrified media birefringent,” *Philos. Mag. J. Sci.* **50**, 337–348 (1875).
- ⁴J. Kerr, “Liv. a new relation between electricity and light: Dielectrified media birefringent (second paper),” *Philos. Mag. J. Sci.* **50**, 446–458 (1875).
- ⁵B. W. Wessels, “Ferroelectric epitaxial thin films for integrated optics,” *Annu. Rev. Mater. Res.* **37**, 659–679 (2007).
- ⁶S. Abel, S. Thilo, C. Marchiori, C. Rossel, M. D. Rossell, R. Erni, D. Caimi, M. Sousa, A. Chelnokov, B. J. Offrein, and J. Fompeyrine, “A strong electro-optically active lead-free ferroelectric integrated on silicon,” *Nat. Commun.* **4** (2013), 10.1038/ncomms2695.
- ⁷M. Zgonik, P. Bernasconi, M. Duelli, R. Schlessler, P. Günter, M. H. Garrett, D. Rytz, Y. Zhu, and X. Wu, “Dielectric, elastic, piezoelectric, electro-optic, and elasto-optic tensors of BaTiO₃ crystals,” *Phys. Rev. B* **50**, 5941–5949 (1994).
- ⁸C. Xiong, W. H. P. Pernice, J. H. Ngai, J. W. Reiner, D. Kumah, F. J. Walker, C. H. Ahn, and H. X. Tang, “Active Silicon Integrated Nanophotonics: Ferroelectric BaTiO₃ Devices,” *Nano Letters* **14**, 1419–1425 (2014).
- ⁹K. J. Kormondy, S. Abel, F. Fallegger, Y. Popoff, P. Ponath, A. B. Posadas, M. Sousa, D. Caimi, H. Siegart, E. Uccelli, L. Czornomaz, C. Marchiori, J. Fompeyrine, and A. A. Demkov, “Analysis of the pockels effect in ferroelectric barium titanate thin films on si(001),” *Microelectronic Engineering* **147**, 215–218 (2015).

- ¹⁰E. H. Turner, “High-frequency electro-optic coefficients of lithium niobate,” *Appl. Phys. Lett.* **8**, 303–304 (1966).
- ¹¹E. Wooten, K. Kissa, A. Yi-Yan, E. Murphy, D. Lafaw, P. Hallemeier, D. Maack, D. Attanasio, D. Fritz, G. McBrien, and D. Bossi, “A review of lithium niobate modulators for fiber-optic communications systems,” *IEEE J. Sel. Top Quantum Electron.* **6**, 69–82 (2000).
- ¹²C. Paillard, S. Prokhorenko, and L. Bellaiche, “Strain engineering of electro-optic constants in ferroelectric materials,” *npj Comput. Mater.* **5** (2019), 10.1038/s41524-018-0141-4.
- ¹³Z. Jiang, C. Paillard, H. O. H. Churchill, M. Xia, S. Zhang, H. Xiang, and L. Bellaiche, “Large linear and nonlinear electro-optic coefficients in two-dimensional ferroelectrics,” *Phys. Rev. B* **106**, L081404–L081410 (2022).
- ¹⁴T. S. Böske, J. Müller, D. Bräuhäus, U. Schröder, and U. Böttger, “Ferroelectricity in hafnium oxide thin films,” *Appl. Phys. Lett.* **99**, 102903 (2011).
- ¹⁵T. S. Böske, J. Müller, D. Bräuhäus, U. Schröder, and B. U., “Ferroelectricity in hafnium oxide: Cmos compatible ferroelectric field effect transistors,” in *2011 International Electron Devices Meeting* (2011) pp. 24.5.1–24.5.4.
- ¹⁶F. Delodovici, P. Barone, and S. Picozzi, “Finite-size effects on ferroelectricity in rhombohedral HfO_2 ,” *Physical Review B* **106**, 115438 (2022).
- ¹⁷F. Delodovici, P. Barone, and S. Picozzi, “Trilinear-coupling-driven ferroelectricity in HfO_2 ,” *Physical Review Materials* **5**, 064405 (2021).
- ¹⁸S. Estandía, N. Dix, J. Gazquez, I. Fina, J. Lyu, M. F. Chisholm, J. Fontcuberta, and F. Sánchez, “Engineering Ferroelectric $\text{Hf}_{0.5}\text{Zr}_{0.5}\text{O}_2$ Thin Films by Epitaxial Stress,” *ACS Appl. Electron. Mater.* , 1449–1457 (2019).
- ¹⁹S. Estandía, N. Dix, M. F. Chisholm, I. Fina, and F. Sánchez, “Domain-Matching Epitaxy of Ferroelectric $\text{Hf}_{0.5}\text{Zr}_{0.5}\text{O}_2(111)$ on $\text{La}_{2/3}\text{Sr}_{1/3}\text{MnO}_3(001)$,” *Cryst. Growth Des.* **20**, 3801–3806 (2020).
- ²⁰Y. Qi, S. Singh, C. Lau, F.-T. Huang, X. Xu, F. J. Walker, C. H. Ahn, S.-W. Cheong, and K. M. Rabe, “Stabilization of Competing Ferroelectric Phases of HfO_2 under Epitaxial Strain,” *Phys. Rev. Lett.* **125**, 257603–257609 (2020).
- ²¹T. D. Huan, V. Sharma, G. A. Rossetti, and R. Ramprasad, “Pathways towards ferroelectricity in hafnia,” *Phys. Rev. B* **90**, 064111–0.64116 (2014).
- ²²Y. Wei, P. Nukala, M. Salverda, S. Matzen, H. J. Zhao, J. Momand, A. S. Everhardt, G. Agnus, G. R. Blake, P. Lecoeur, B. J. Kooi, J. Íñiguez, B. Dkhil, and B. Noheda, “A rhombohedral

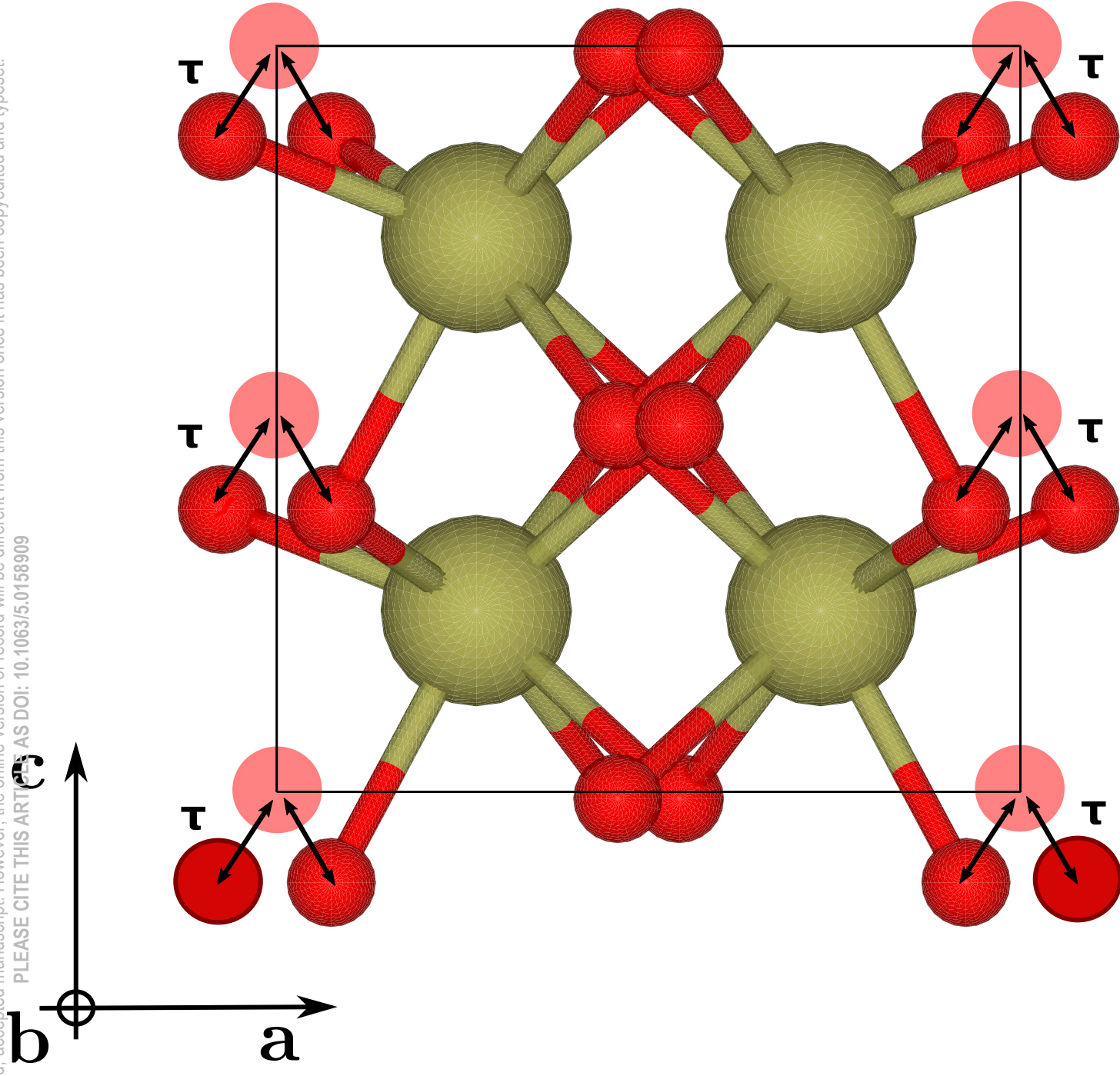
- ferroelectric phase in epitaxially strained $\text{Hf}_{0.5}\text{Zr}_{0.5}\text{O}_2$ thin films,” *Nature Mater.* **17** (2018), 10.1038/s41563-018-0196-0.
- ²³P. Nukala, J. Antoja-Lleonart, Y. Wei, L. Yedra, B. Dkhil, and B. Noheda, “Direct Epitaxial Growth of Polar $(1-x)\text{HfO}_2-(x)\text{ZrO}_2$ Ultrathin Films on Silicon,” *ACS Appl. Electron. Mater.* **1**, 2585–2593 (2019).
- ²⁴Y. Zhang, Q. Yang, L. Tao, E. Y. Tsymlal, and V. Alexandrov, “Effects of Strain and Film Thickness on the Stability of the Rhombohedral Phase of HfO_2 ,” *Phys. Rev. Appl.* **14**, 014068–014076 (2020).
- ²⁵S. S. Cheema, N. Shanker, C.-H. Hsu, A. Datar, J. Bae, D. Kwon, and S. Salahuddin, “One Nanometer HfO_2 -Based Ferroelectric Tunnel Junctions on Silicon,” *Adv. Electron. Mater.* **8**, 2100499 (2022).
- ²⁶I. Fina and F. Sánchez, “Epitaxial Ferroelectric HfO_2 Films: Growth, Properties, and Devices,” *ACS Appl. Electron. Mater.* **3** (2021), 10.1021/acsaelm.1c00110.
- ²⁷M. H. Park, Y. H. Lee, H. J. Kim, Y. J. Kim, T. Moon, K. D. Kim, J. Müller, A. Kersch, U. Schroeder, T. Mikolajick, and C. S. Hwang, “Ferroelectricity and Antiferroelectricity of Doped Thin HfO_2 -Based Films,” *Adv. Mater.* **27**, 1811–1831 (2015).
- ²⁸S. E. Reyes-Lillo, K. F. Garrity, and K. M. Rabe, “Antiferroelectricity in thin-film ZrO_2 from first principles,” *Phys. Rev. B* **90**, 140103–140108 (2014).
- ²⁹P. D. Lomenzo, M. Materano, T. Mittmann, P. Buragohain, A. Gruverman, T. Kiguchi, T. Mikolajick, and U. Schroeder, “Harnessing Phase Transitions in Antiferroelectric ZrO_2 Using the Size Effect,” *Adv. Electron. Mater.* **8**, 2100556 (2022).
- ³⁰D. Lehninger, D. Rafaja, J. Wünsche, F. Schneider, J. von Borany, and J. Heitmann, “Formation of orthorhombic $(\text{Zr,Ta})\text{O}_2$ in thin Zr-Ta-O films,” *Appl. Phys. Lett.* **110** (2017), 10.1063/1.4990529.
- ³¹S. Kondo, R. Shimura, T. Teranishi, A. Kishimoto, T. Nagasaki, H. Funakubo, and T. Yamada, “Linear electro-optic effect in ferroelectric HfO_2 -based epitaxial thin films,” *Jpn. J. Appl. Phys.* **60**, 070905 (2021).
- ³²A. El Boutaybi, P. Karamanis, T. Maroutian, S. Matzen, L. Vivien, P. Lecoeur, and M. Rérat, “Electro-optic properties of ZrO_2 , HfO_2 , and LiNbO_3 ferroelectric phases: A comparative density functional study,” *Phys. Rev. B* **107**, 045140–045150 (2023).
- ³³S. Liu and B. M. Hanrahan, “Effects of growth orientations and epitaxial strains on phase stability of HfO_2 thin films,” *Phys. Rev. Mater.* **3**, 054404 (2019).

- ³⁴M. Hoffmann, U. Schroeder, T. Schenk, T. Shimizu, H. Funakubo, O. Sakata, D. Pohl, M. Drescher, C. Adelman, R. Materlik, A. Kersch, and T. Mikolajick, “Stabilizing the ferroelectric phase in doped hafnium oxide,” *J. Appl. Phys.* **118**, 072006 (2015).
- ³⁵R. Batra, T. D. Huan, J. L. Jones, G. J. Rossetti, and R. Ramprasad, “Factors favoring ferroelectricity in hafnia: A first-principles computational study,” *J. Phys. Chem. C* **121**, 4139–4145 (2017).
- ³⁶U. Schröder, C. Richter, M. H. Park, T. Schenk, M. Pešić, M. Hoffmann, F. P. G. Fengler, D. Pohl, B. Rellinghaus, C. Zhou, C.-C. Chung, J. L. Jones, and T. Mikolajick, “Lanthanum-doped hafnium oxide: A robust ferroelectric material,” *Inorg. Chem.* **57**, 2752–2765 (2018).
- ³⁷P. Nukala, M. Ahmadi, Y. Wei, S. de Graaf, E. Stylianidis, T. Chakraborty, S. Matzen, H. W. Zandbergen, A. Björling, D. Mannix, D. Carbone, B. Kooi, and B. Noheda, “Reversible oxygen migration and phase transitions in hafnia-based ferroelectric devices,” *Science* **372**, 630–635 (2021).
- ³⁸R. He, H. Wu, S. Liu, H. Liu, and Z. Zhong, “Ferroelectric structural transition in hafnium oxide induced by charged oxygen vacancies,” *Phys. Rev. B* **104**, L180102–L180108 (2021).
- ³⁹M. Veithen, X. Gonze, and P. Ghosez, “First-principles study of the electro-optic effect in ferroelectric oxides,” *Phys. Rev. Lett.* **93**, 187401 (2004).
- ⁴⁰M. Veithen, X. Gonze, and P. Ghosez, “Nonlinear optical susceptibilities, raman efficiencies, and electro-optic tensors from first-principles density functional perturbation theory,” *Phys. Rev. B* **71**, 125107–125121 (2005).
- ⁴¹X. Gonze, B. Amadon, P.-M. Anglade, J.-M. Beuken, F. Bottin, P. Boulanger, F. Bruneval, D. Caliste, R. Caracas, M. Côté, T. Deutsch, L. Genovese, P. Ghosez, M. Giantomassi, S. Goedecker, D. Hamann, P. Hermet, F. Jollet, G. Jomard, S. Leroux, M. Mancini, S. Mazevet, M. Oliveira, G. Onida, Y. Pouillon, T. Rangel, G.-M. Rignanese, D. Sangalli, R. Shaltaf, M. Torrent, M. Verstraete, G. Zerah, and J. Zwanziger, “Abinit: First-principles approach to material and nanosystem properties,” *Comput. Phys. Commun.* **180**, 2582–2615 (2009).
- ⁴²X. Gonze, “First-principles responses of solids to atomic displacements and homogeneous electric fields: Implementation of a conjugate-gradient algorithm,” *Phys. Rev. B* **55**, 10337–10354 (1997).
- ⁴³J. P. Perdew and A. Zunger, “Self-interaction correction to density-functional approximations for many-electron systems,” *Phys. Rev. B* **23**, 5048–5079 (1981).

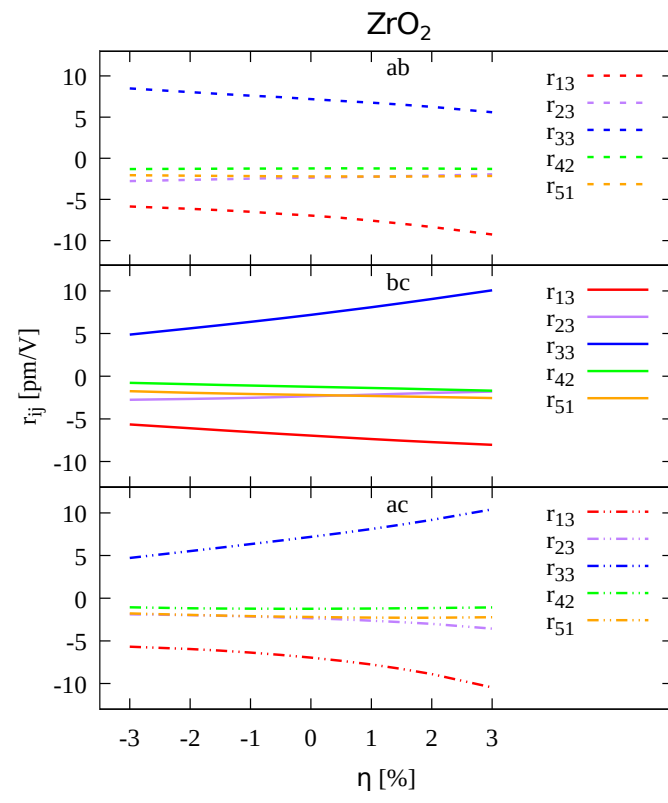
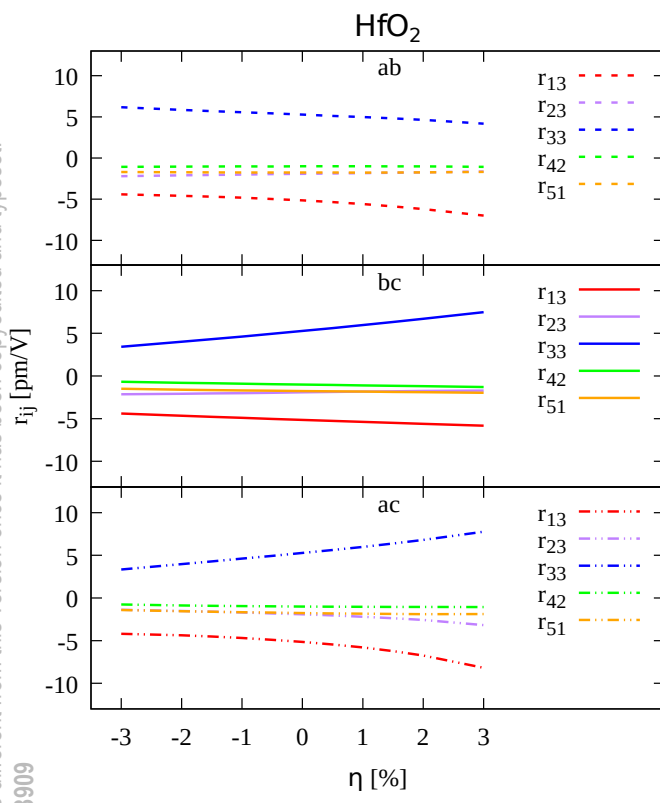
- ⁴⁴M. I. Aroyo, A. Kirov, C. Capillas, J. Perez-Mato, and H. Wondratschek, “Bilbao crystallographic server. ii. representations of crystallographic point groups and space groups,” *Acta Crystallogr. Sect. A Found. Crystallogr.* **62**, 115–128 (2006).
- ⁴⁵J. F. Nye *et al.*, *Physical properties of crystals: their representation by tensors and matrices* (Oxford university press, 1985).
- ⁴⁶Z. Jiang, C. Paillard, D. Vanderbilt, H. Xiang, and L. Bellaiche, “Designing Multifunctionality via Assembling Dissimilar Materials: Epitaxial AlN/ScN Superlattices,” *Physical Review Letters* **123**, 096801 (2019).
- ⁴⁷Z. Jiang, C. Paillard, H. Xiang, and L. Bellaiche, “Linear Versus Nonlinear Electro-Optic Effects in Materials,” *Physical Review Letters* **125**, 017401 (2020).
- ⁴⁸I. Petousis, D. Mrdjenovich, E. Ballouz, M. Liu, D. Winston, W. Chen, T. Graf, T. D. Schladt, K. A. Persson, and F. B. Prinz, “High-throughput screening of inorganic compounds for the discovery of novel dielectric and optical materials,” *Sci. Data* **4**, 1–12 (2017).
- ⁴⁹P. Zubko, J. C. Wojdeł, M. Hadjimichael, S. Fernandez-Pena, A. Sené, I. Luk’yanchuk, J.-M. Triscone, and J. Íñiguez, “Negative capacitance in multidomain ferroelectric superlattices,” *Nature* **534**, 524–528 (2016).
- ⁵⁰J. Íñiguez, P. Zubko, I. Luk’yanchuk, and A. Cano, “Ferroelectric negative capacitance,” *Nature Reviews Materials* **4**, 243 (2019).
- ⁵¹J. Müller, P. Polakowski, S. Mueller, and T. Mikolajick, “Ferroelectric hafnium oxide based materials and devices: Assessment of current status and future prospects,” *ECS Journal of Solid State Science and Technology* **4**, N30 (2015).
- ⁵²S. Migita, H. Ota, H. Yamada, A. Sawa, and A. Toriumi, “Thickness-independent behavior of coercive field in HfO₂-based ferroelectrics,” in *2017 IEEE Electron Devices Technology and Manufacturing Conference (EDTM)* (IEEE, 2017) pp. 255–256.
- ⁵³J. Müller, P. Polakowski, S. Mueller, and T. Mikolajick, “Ferroelectric Hafnium Oxide Based Materials and Devices: Assessment of Current Status and Future Prospects,” *ECS Journal of Solid State Science and Technology* **4**, N30–N35 (2015).

This is the author's peer reviewed, accepted manuscript. However, the online version of record will be different from this version once it has been copyedited and typeset.

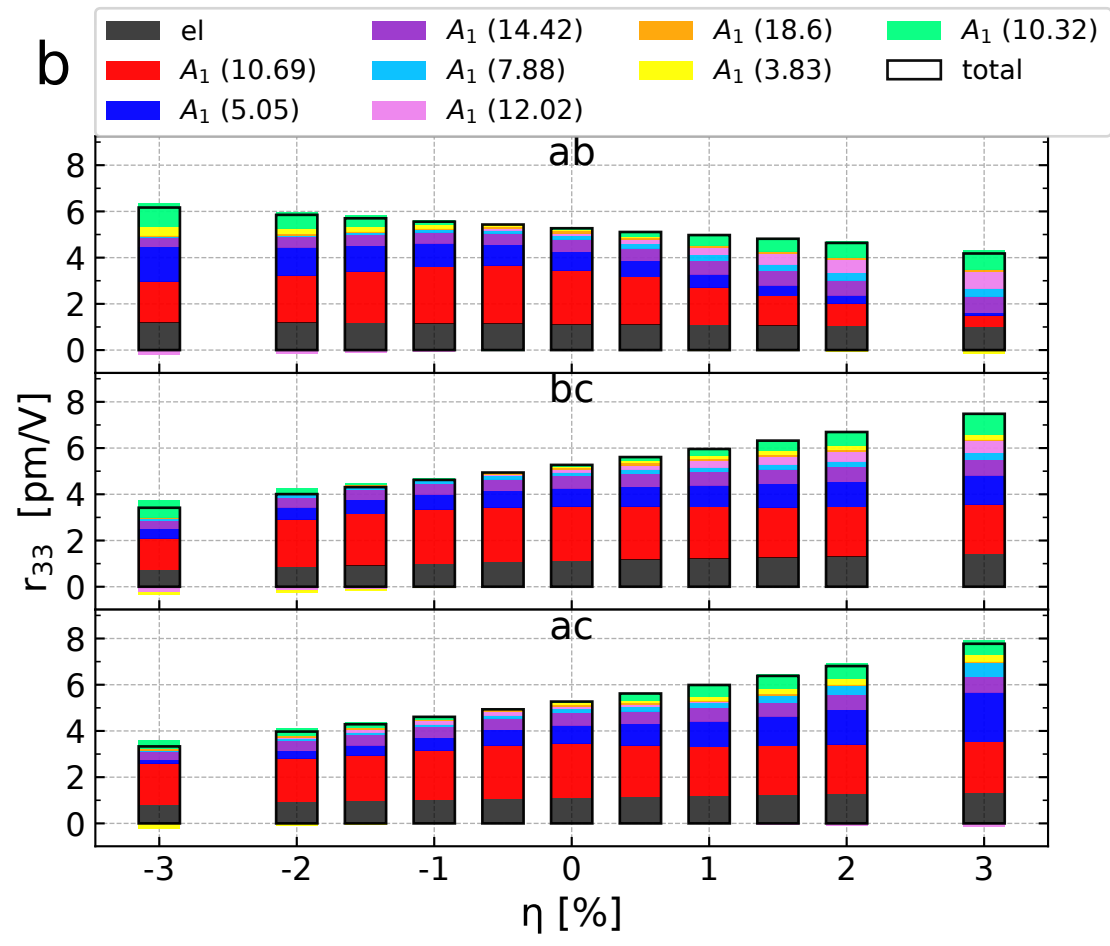
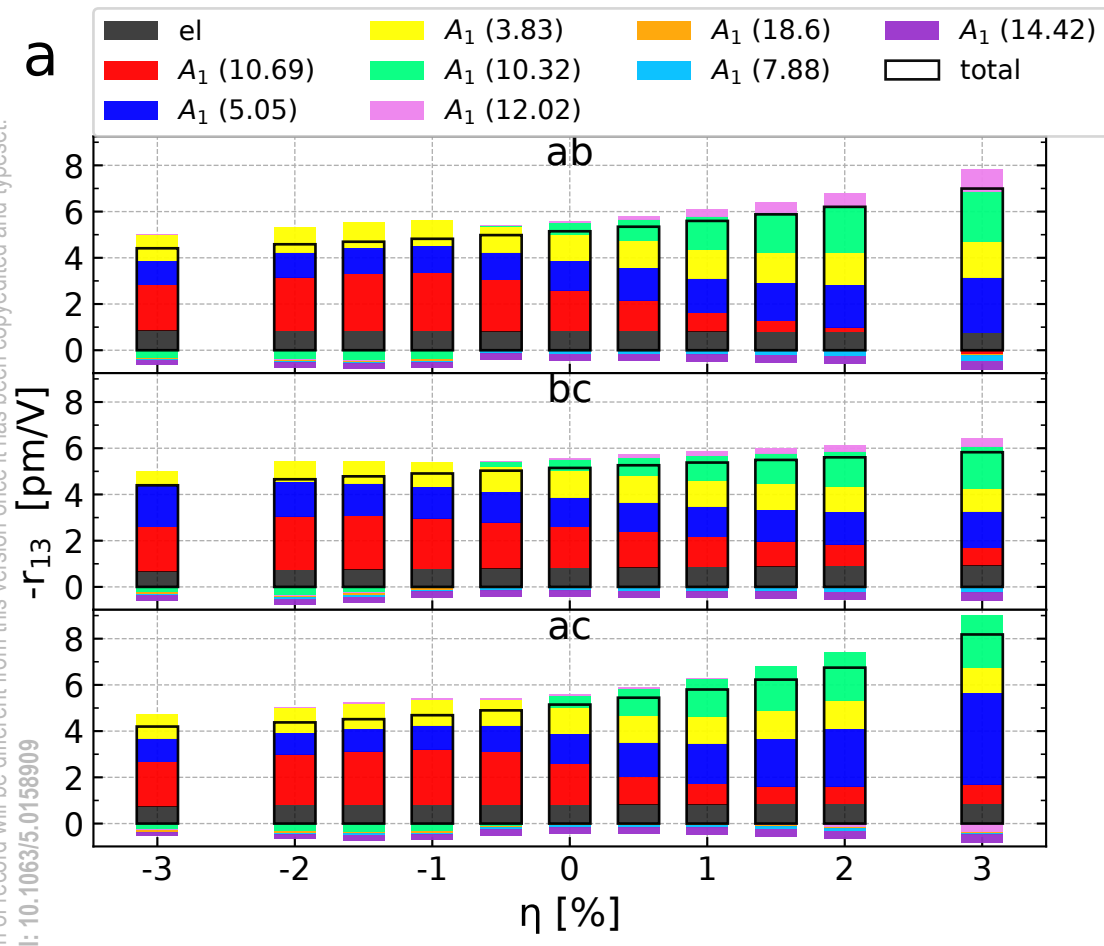
PLEASE CITE THIS ARTICLE AS DOI: 10.1063/5.0158909



This is the author's peer reviewed, accepted manuscript. However, the online version of record will be different from this version once it has been copyedited and typeset.
PLEASE CITE THIS ARTICLE AS DOI: 10.1063/5.0158909



This is the author's peer reviewed, accepted manuscript. However, the online version of record will be different from this version once it has been copyedited and typeset.
PLEASE CITE THIS ARTICLE AS DOI: 10.1063/5.0158909



This is the author's peer reviewed, accepted manuscript. However, the online version of record will be different from this version once it has been copyedited and typeset.
PLEASE CITE THIS ARTICLE AS DOI: 10.1063/5.0158909

